G-actin regulates the shuttling and PP1 binding of the RPEL protein Phactr1 to control actomyosin assembly

Maria Wiezlak[1], Jessica Diring[1,*], Jasmine Abella[2,*], Stephane Mouilleron[1,3,*], Michael Way[2], Neil Q. McDonald[3,4] and Richard Treisman[1,‡]

[1]Transcription Group, CRUK London Research Institute, 44 Lincoln's Inn Fields, London WC2A 3LY, UK
[2]Cell Motility Group, CRUK London Research Institute, 44 Lincoln's Inn Fields, London WC2A 3LY, UK
[3]Structural Biology Group, CRUK London Research Institute, 44 Lincoln's Inn Fields, London WC2A 3LY, UK
[4]Institute of Structural and Molecular Biology, Department of Biological Sciences, Birkbeck College, University of London, Malet Street, London WC1E 7HX, UK

*These authors contributed equally to this work
‡Author for correspondence (richard.treisman@cancer.org.uk)

Accepted 14 August 2012
Journal of Cell Science 125, 5860–5872

doi: 10.1242/jcs.112078

Summary

The Phactr family of PP1-binding proteins is implicated in human diseases including Parkinson's, cancer and myocardial infarction. Each Phactr protein contains four G-actin binding RPEL motifs, including an N-terminal motif, abutting a basic element, and a C-terminal triple RPEL repeat, which overlaps a conserved C-terminus required for interaction with PP1. RPEL motifs are also found in the regulatory domains of the MRTF transcriptional coactivators, where they control MRTF subcellular localisation and activity by sensing signal-induced changes in G-actin concentration. However, whether G-actin binding controls Phactr protein function – and its relation to signalling – has not been investigated. Here, we show that Rho-actin signalling induced by serum stimulation promotes the nuclear accumulation of Phactr1, but not other Phactr family members. Actin binding by the three Phactr1 C-terminal RPEL motifs is required for Phactr1 cytoplasmic localisation in resting cells. Phactr1 nuclear accumulation is importin α-β dependent. G-actin and importin α-β bind competitively to nuclear import signals associated with the N- and C-terminal RPEL motifs. All four motifs are required for the inhibition of serum-induced Phactr1 nuclear accumulation when G-actin is elevated. G-actin and PP1 bind competitively to the Phactr1 C-terminal region, and Phactr1 C-terminal RPEL mutants that cannot bind G-actin induce aberrant actomyosin structures dependent on their nuclear accumulation and on PP1 binding. In CHL-1 melanoma cells, Phactr1 exhibits actin-regulated subcellular localisation and is required for stress fibre assembly, motility and invasiveness. These data support a role for Phactr1 in actomyosin assembly and suggest that Phactr1 G-actin sensing allows its coordination with F-actin availability.

Key words: Actin, Phactr, RPEL, PP1, Actomyosin

Introduction

Actin-binding proteins play well defined roles in the regulation of actin dynamics and regulated assembly of F-actin based structures involved in cell motility and adhesion (Narumiya et al., 2009; Dominguez and Holmes, 2011; Spiering and Hodgson, 2011). In addition, actin and its binding partners are involved in extra-cytoskeletal processes, including transcriptional regulation, chromatin remodelling and modification, and RNA processing (Gieni and Hendzel, 2009; Zheng et al., 2009). Perhaps the best understood of these functions is the role of G-actin in control of nucleocytoplasmic shuttling and transcriptional activation by the MRTF family of SRF transcriptional coactivators (Miralles et al., 2003; Vartiainen et al., 2007). Signal-induced changes in the availability of G-actin regulate the assembly of different G-actin complexes on the MRTF regulatory domain, which contains three G-actin binding RPEL motifs (Mouilleron et al., 2008; Hirano and Matsuura, 2011; Mouilleron et al., 2011).

RPEL motifs are also found in the four Phactr (phosphatase and actin regulator) proteins (Sagara et al., 2003; Allen et al., 2004), whose biochemical functions and biological significance remain obscure. Each Phactr protein contains a conserved N-terminal region comprising a basic element abutting a single RPEL motif, together with a triple RPEL repeat preceding conserved C-terminal sequences required for PP1 binding (Fig. 1A; Sagara et al., 2003; Allen et al., 2004; Kim et al., 2007). In humans, Phactr1 has been implicated in melanoma progression, early-onset myocardial infarct, and endothelial cell tube formation (Smith et al., 2005; Kathiresan et al., 2009; Koh et al., 2009; Trufant, 2010; Jarray et al., 2011); Phactr2 in Parkinson's disease (Wider et al., 2009); and Phactr3 in non-small cell lung cancer (Bankovic et al., 2010). In the mouse, the Phactr4 *humdy* mutation abolishes Phactr4–PP1 interaction and causes defective neural tube closure and enteric neural crest cell migration, reflecting increased Rb-E2F1 activity and focal adhesion-based Rho-ROCK signalling respectively (Kim et al., 2007; Zhang et al., 2012).

The relevance of G-actin binding to Phactr functions such as PP1 binding remains unclear, but the conservation of the RPEL and C-terminal sequences between the four Phactr proteins suggests they share a common mode of regulation. In Phactr3, sequences required for high-affinity PP1 binding overlap its RPEL3 motif (Sagara et al., 2003), suggesting that actin and PP1 might compete for Phactr binding. Actin binding appears

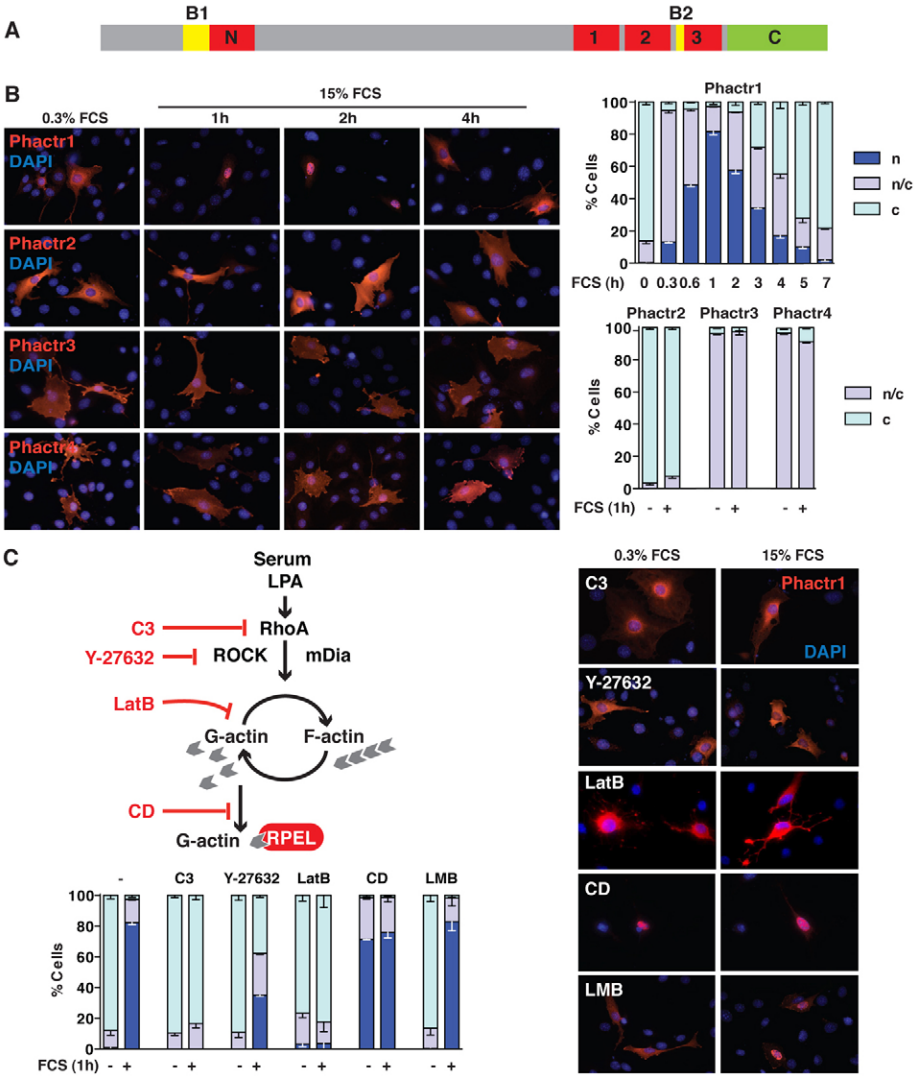

Fig. 1. Phactr1 subcellular localisation is controlled by Rho-actin signalling. (**A**) Protein sequence elements in the Phactr family of proteins. Yellow, conserved basic elements; red, RPEL motifs (pfam PF02755); green, C-terminal region. (**B**) NIH3T3 cells expressing FLAG-tagged Phactr proteins were maintained in 0.3% serum for 24 hours, then stimulated with 15% serum for 1 hour, 2 hours and 4 hours. Localisation of the proteins was visualised by fluorescence microscopy and is summarised on the right (C, cytoplasmic; N/C, pancellular; N, nuclear; at least 75 cells counted per point, error bars represent the s.e.m. of three independent experiments). (**C**) Upper left, schematic of the Rho-actin signal pathway, indicating points of action of the various inhibitors used. Right, effects of inhibitors on serum-induced nuclear accumulation of FLAG-tagged Phactr1, either co-expressed with C3 transferase, or following pretreatment with Y-27632, latrunculin B (LatB), cytochalasin D (CD) or the Crm1 exportin inhibitor leptomycin B (LMB). Lower left, summary of the data.

required for morphological changes induced by Phactr3 overexpression, and in some systems PP1 binding is also required (Sagara et al., 2009; Farghaian et al., 2011). Phactr3 inhibits PP1 activity against a model substrate (Sagara et al., 2003), but it remains unclear whether this reflects a bona fide general inhibitory function of Phactr3 or a positive function as a regulatory subunit for a different substrate (for discussion see Ceulemans and Bollen, 2004; Roy and Cyert, 2009). Phactr1 and Phactr3 have been detected in cell nuclei, but whether they exhibit regulated nucleocytoplasmic shuttling has not been investigated (Sagara et al., 2003; Allen et al., 2004; Favot et al., 2005; Farghaian et al., 2011).

Here we show that in fibroblasts Phactr1, but not Phactrs 2, 3 or 4, exhibits actin-regulated nucleocytoplasmic shuttling, and that in resting cells, Phactr1 cytoplasmic localisation is critically dependent on the C-terminal RPEL repeat. G-actin competes with PP1 for binding to the C-terminal region and with importin α-β for two nuclear import signals associated with the N- and C-terminal RPEL motifs. In the nucleus, actin-free Phactr1 induces formation of aberrant actomyosin structures in a PP1-dependent fashion. In CHL-1 melanoma cells, endogenous Phactr1 also exhibits actin-regulated subcellular localisation, and is required for stress fibre assembly, motility and invasive behaviour.

Results

Phactr1 subcellular localisation is controlled by Rho-actin signalling

We used transient transfection in NIH3T3 fibroblasts to test whether Phactr proteins exhibit nuclear accumulation in fibroblasts following serum stimulation, as previously observed with the MRTFs (Miralles et al., 2003; Vartiainen et al., 2007). In serum-deprived cells, transiently expressed Phactr1 was predominantly cytoplasmic and Phactr2 almost exclusively so, while Phactr3 and Phactr4 exhibited pancellular staining (Fig. 1B). Upon serum stimulation, Phactr1 accumulated in cell nuclei within 1 hour, before reappearing in the cytoplasm over a subsequent 6-hour period, while the subcellular localisation of Phactr2, Phactr3 and Phactr4 remained unaffected (Fig. 1B; supplementary material Fig. S1).

Nuclear accumulation of transiently expressed Phactr1 was inhibited by C3 transferase, which specifically inactivates Rho, and less effectively by Y27632, which inhibits the Rho effector kinase ROCK (Fig. 1C). Treatment of cells with latrunculin B,

which prevents actin polymerisation but not actin:RPEL interaction, blocked serum-induced Phactr1 nuclear accumulation; by contrast, cytochalasin D, which prevents actin:RPEL interaction, induced Phactr1 nuclear localisation in the absence of serum stimulation (Fig. 1C). These results indicate that Phactr1 subcellular localisation is controlled by the Rho-actin signal pathway, which also controls the MRTFs (Sotiropoulos et al., 1999; Miralles et al., 2003). The MRTFs are predominantly nuclear when expressed in MDA-MB-231 breast cancer cells, and Phactr1 also exhibited predominantly nuclear or pancellular localisation, indicating that both proteins respond similarly to different basal levels of Rho-actin signalling (supplementary material Fig. S2). In contrast to the MRTFs, however, treatment with the Crm1 inhibitor leptomycin B did not induce nuclear accumulation of Phactr1, indicating the Crm1 exportin is not essential for Phactr1 nuclear export (Fig. 1C) (Vartiainen et al., 2007).

Serum-induced Phactr1 nuclear accumulation requires the C-terminal RPEL motifs

Having demonstrated that Rho-actin signalling controls the subcellular localisation of Phactr1, we focused our attention on this member of the family. First, we used fluorescence polarisation anisotropy to determine the actin-binding affinities of fluorescently labelled Phactr1 RPEL peptides encompassing each RPEL motif. Latrunculin B–actin (LatB–actin) bound the Phactr1 RPEL motifs with affinities ranging from 0.27 μM to 4.34 μM, somewhat more strongly than those from MRTF-A, and R→A substitutions at the motif core reduced binding by one to two orders of magnitude (Fig. 2A). We therefore used R→A substitutions at each motif, or deletions of the N-terminal motif or the C-terminal RPEL repeat, to investigate the role of the RPEL motifs in Phactr1 subcellular localisation.

Deletion of RPEL-N, or R→A substitution of its conserved arginine, had no effect on Phactr1 localisation in either resting or serum-stimulated cells; by contrast, deletion of the C-terminal RPEL repeat, or R→A substitutions in all three C-terminal motifs (Phactr1-xxx), resulted in constitutive Phactr1 nuclear localisation (Fig. 2B). Deletion of the central sequences between RPEL-N and the C-terminal RPEL repeat, or the conserved C-terminal sequence, had no effect (Fig. 2B). These results suggest that the C-terminal RPEL repeat is required to sense signal-induced actin depletion.

We next investigated the role of individual RPEL motifs. Within the C-terminal RPEL repeat, R→A substitutions at RPEL1 (x23) or RPEL2 (1x3) had little effect on Phactr1 localisation in resting cells, but R→A substitution at RPEL3 (12x) caused significant nuclear accumulation (Fig. 2C). Pairwise combination of the C-terminal RPEL1 and RPEL2 R→A mutations slightly increased nuclear accumulation, but combination of either of these mutations with the RPEL3 R→A mutation caused nuclear accumulation in the majority of the cell population (Fig. 2C). As the number of C-terminal R→A mutations increased, the number of cells expressing Phactr1 decreased, suggesting that inactivation of actin binding has a toxic consequence (supplementary material Fig. S3; see below). Combination of the RPEL-N R→A mutation with R→A mutations within the C-terminal cluster had little additional effect (Fig. 2C, right). These results show that all three C-terminal RPEL motifs are required to maintain the cytoplasmic localisation of Phactr1 in resting cells, with RPEL3 playing a dominant role, while the N-terminal RPEL-N motif makes only a minor contribution.

Actin competes with importin α-β to inhibit Phactr1 nuclear import

The Predictprotein algorithm (Rost et al., 2004) identifies a potential bipartite NLS (‘B1’) in the conserved sequences N-terminal to RPEL-N, and a further potential NLS (‘B2’) embedded within the C-terminal RPEL repeat (Fig. 3A). Deletion of B1, or clustered alanine substitution of either of its two basic elements, effectively abolished serum-induced nuclear accumulation of Phactr1 (Fig. 3B). Clustered alanine substitutions within the B2 element, which do not impinge on residues involved in interaction with actin (Mouilleron et al., 2012) also impaired serum-induced Phactr1 nuclear accumulation (Fig. 3B). The B1 and B2 mutations had a less pronounced effect on the constitutive nuclear accumulation of Phactr1-xxx (Fig. 3B), however, suggesting that their inhibition of Phactr1 interaction with the nuclear import machinery is incomplete, or that further nuclear import sequences are present.

RNAi-mediated depletion of importin β1 completely abolished serum-induced Phactr1 nuclear accumulation, suggesting that Phactr1 nuclear import is importin α-β dependent (Fig. 3C). Consistent with this, in pulldown experiments GST-Phactr1 fusion derivatives containing either the N- or C-terminal NLS elements efficiently recovered recombinant importin α-β from solution, and addition of increasing amounts of LatB–actin (G-actin) to the binding reactions effectively competed for binding in both cases (Fig. 3D). Artificial elevation of cellular G-actin concentration prevents MRTF nuclear accumulation and SRF activation (Sotiropoulos et al., 1999; Posern et al., 2002; Miralles et al., 2003). Overexpression of either wild-type actin or the non-polymerising R62D mutant inhibited serum-induced Phactr1 nuclear accumulation, and this required the integrity of both RPEL-N and the C-terminal RPEL repeat (Fig. 3E; supplementary material Fig. S4).

Taken together, these results demonstrate the existence of two importin α-β dependent nuclear import signals in Phactr1 associated with the N- and C-terminal RPEL motifs. Actin competes with importin α-β for binding to these nuclear import signals, as observed with the MRTFs (Pawlowski et al., 2010; Hirano and Matsuura, 2011), and saturation of all the G-actin binding sites in Phactr1 is required for effective inhibition of its nuclear accumulation by actin overexpression (see Discussion).

Actin and PP1 bind competitively to Phactr1

We next investigated Phactr1–PP1 interaction. PP1 was substantially nuclear in resting cells and did not appreciably redistribute upon serum stimulation (Fig. 4A). Transiently expressed Phactr1 is cytoplasmic under these conditions, and its interaction with co-expressed PP1 was barely detectable by co-immunoprecipitation (Fig. 4B). Serum stimulation, which induces nuclear accumulation of Phactr1, significantly increased recovery of Phactr1 in PP1 immunoprecipitates (Fig. 4B). By contrast, interaction between PP1 and Phactr1-xxx, which is constitutively nuclear, was substantially higher than with wild-type Phactr1 and did not increase upon serum stimulation (Fig. 4B). Phactr1 lacking its RPEL domain did not bind PP1, even though it was constitutively nuclear, while deletion of the conserved C-terminal region abolished PP1 interaction of both wild-type Phactr1 and Phactr1-xxx (Fig. 4C).

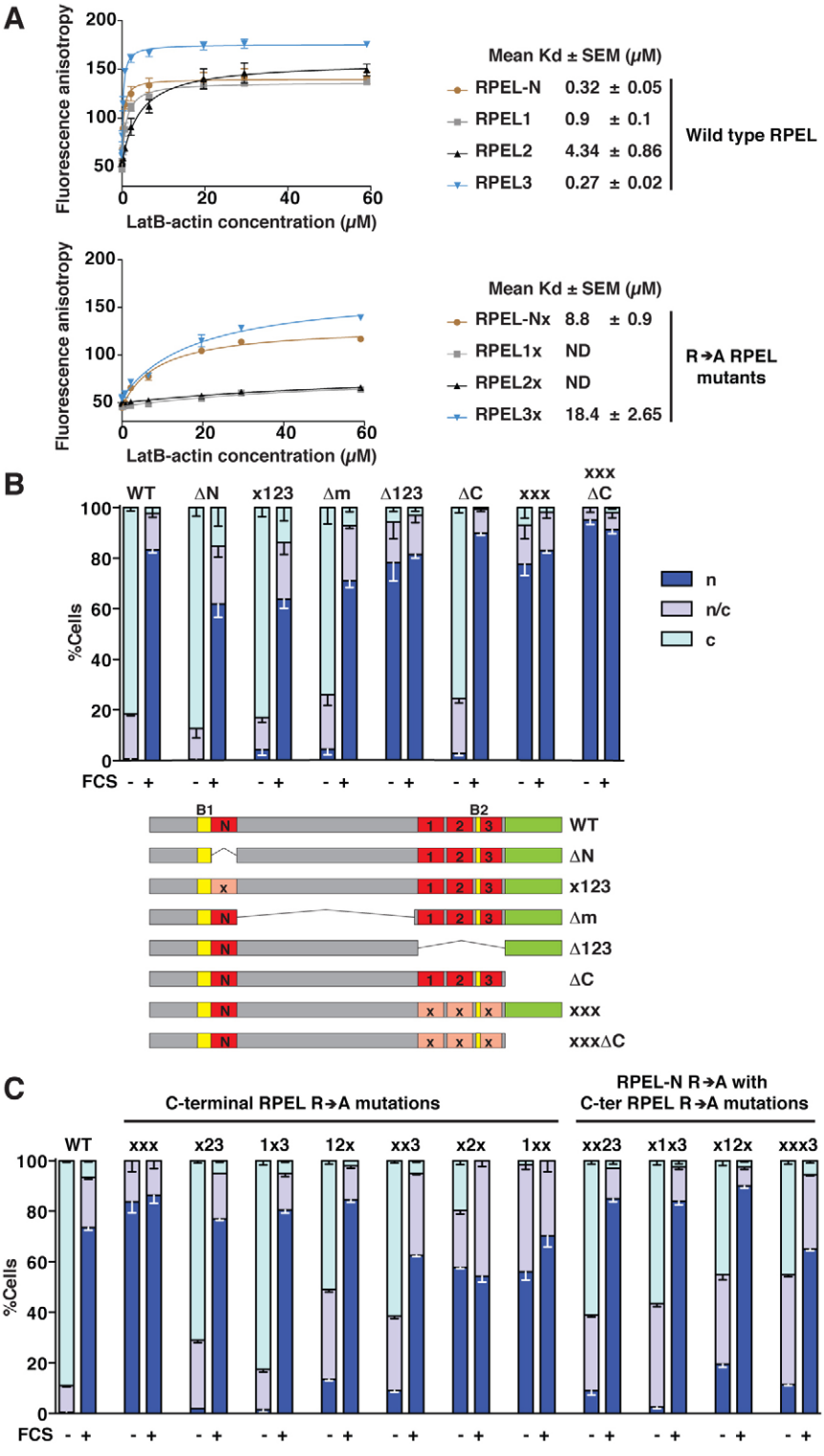

Fig. 2. Serum-induced Phactr1 nuclear accumulation requires the C-terminal RPEL motifs. (**A**) Fluorescence anisotropy measurement of G-actin binding by the four Phactr1 RPEL motifs. Anisotropies of FITC-conjugated 32-amino acid RPEL peptides (0.5 μM) were measured over a range of LatB–actin concentrations. Graphs correspond to one of three experiments performed in duplicate. Dissociation constants (K_d) are means of three independent experiments ± s.e.m. ND, binding not detectable. (**B**) Localisation of Phactr1 deletion and point mutants in resting and serum-stimulated cells was visualised by fluorescence microscopy and scored as in Fig. 1B (C, cytoplasmic; N/C, pancellular; N, nuclear). The Phactr1 derivatives are shown schematically below. WT, wild-type. R→A mutations in the RPEL motifs are indicated by 'x'. (**C**) RPEL3 plays a dominant role in signal-induced Phactr1 nuclear accumulation. Localisation in resting and serum-stimulated cells of Phactr1 derivatives carrying RPEL motif R→A mutations, singly and in combination, was scored as in Fig. 1B.

These results show that the sequences required for PP1 binding include both the C-terminal conserved region and sequences within the RPEL repeat, consistent with a previous study of Phactr3 (Sagara et al., 2003), and suggest that actin may compete with PP1 for Phactr1 binding. To test this directly, we co-expressed the GST-Phactr1 C-terminal fusion protein and PP1 in bacteria, and incubated the GST-Phactr1–PP1 with increasing concentrations of G-actin. Increasing amounts of LatB–actin effectively competed for PP1 binding, and this was substantially impaired in the presence of cytochalasin D, whose binding site on actin overlaps that of the RPEL motif (Fig. 4D) (Vartiainen et al., 2007; Mouilleron et al., 2008; Nair et al., 2008). Actin and PP1 thus compete for binding to Phactr1. We note that in serum-stimulated cells, the interaction between PP1 and wild-type

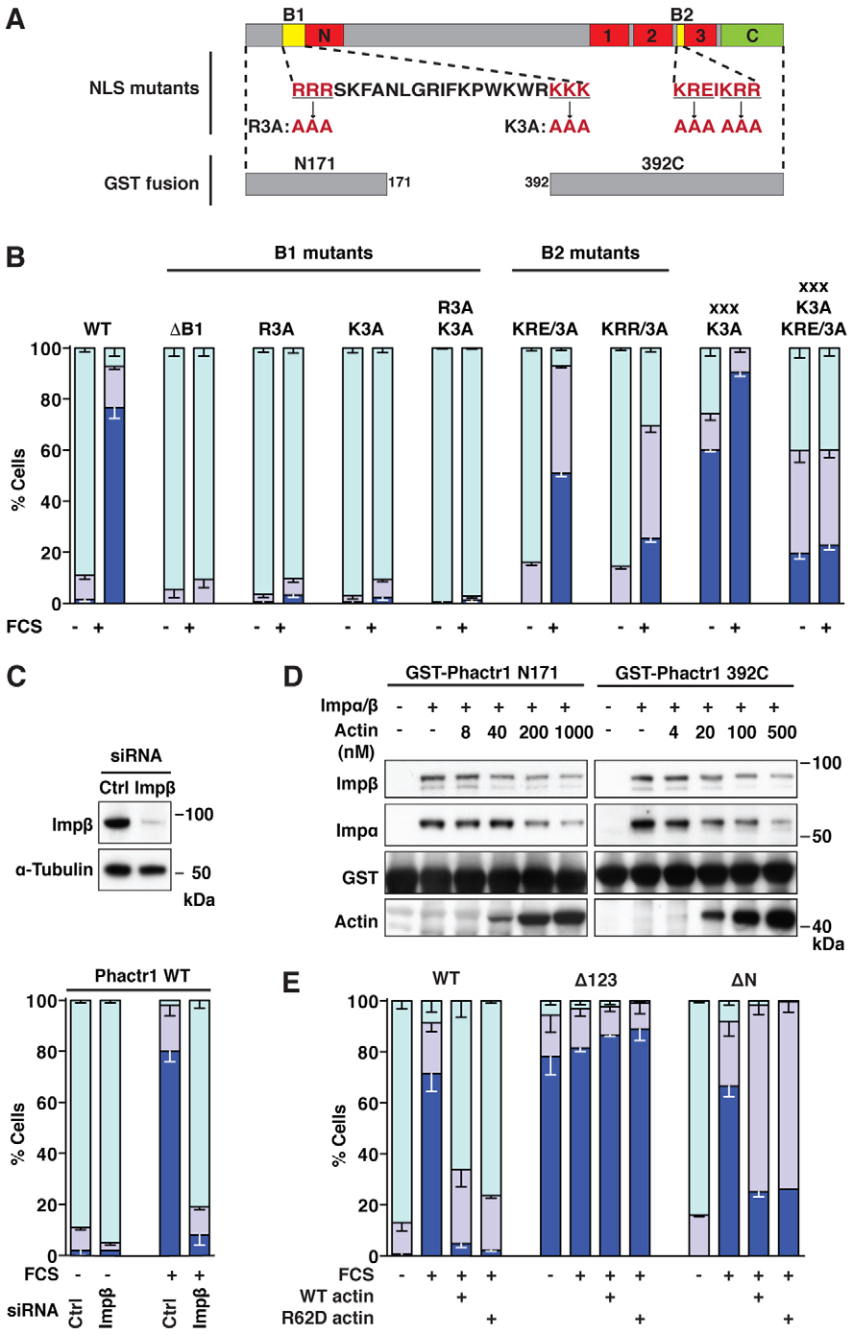

Fig. 3. Phactr1 contains two actin-regulated importin α-β dependent nuclear import signals. (**A**) Schematic representation of Phactr1 as in Figure 1A, showing wild-type and mutant Phactr1 nuclear localisation signals B1 and B2, and the GST fusion proteins used. (**B**) Localisation of different Phactr1 NLS mutants in resting and serum-stimulated cells was assessed as in Fig. 1B. WT, wild-type. (**C**) Importin β (Impβ) activity is required for Phactr1 nuclear accumulation in NIH3T3 cells. Top, western blot showing depletion of Impβ. Bottom, localisation of wild-type Phactr1 in resting and serum-stimulated cells with or without Impβ depletion, scored as in Fig. 1B. (**D**) Actin competes with Impα3–Impβ for binding to the Phactr1 N- and C-termini. GST-Phactr1 fusion derivatives containing either the N- or C-terminal NLS elements (GST-Phactr1 N171 and GST-Phactr1 392C, panel A) were used for pulldown of recombinant Impα3–Impβ in the presence of increasing amounts of latB–actin. Bound proteins were analysed by immunoblotting. (**E**) Both N- and C-terminal RPEL motifs are required for inhibition of Phactr1 nuclear accumulation by actin overexpression. The indicated Phactr1 derivatives were co-expressed with wild-type actin or nonpolymerisable actin R62D and their localisation before and after serum stimulation scored as in Fig. 1B.

Phactr1 remains less efficient than that with Phactr1-xxx, suggesting that even under stimulated conditions G-actin concentrations are sufficient to compete effectively with PP1 for Phactr1 (Fig. 4B).

Activated Phactr1–PP1 binding induces aberrant actomyosin structures

During our analysis of RPEL motif mutants, we noted that expression of nuclear Phactr1 induced rearrangements of the fibroblast actin cytoskeleton, with many cells exhibiting intense F-actin foci or grossly thickened stress fibres, which also contained myosin regulatory light chain (MLC) (Fig. 5A; supplementary material Fig. S5). These phenotypes are reminiscent of cells expressing the catalytic domain of the Rho effector kinase ROCK (Leung et al., 1996; Sahai et al., 1998) and may explain the reduced numbers of cells expressing Phactr1 C-terminal RPEL R→A mutants (supplementary material Fig. S3). Both F-actin phenotypes were induced by constitutively nuclear Phactr1-xxx but not by the Phactr1-xxx C-terminal deletion mutant, indicating that they are dependent on the interaction of Phactr1 with PP1 (Fig. 5A; supplementary material Figs S6, S7).

To gain insight into the relationship between Phactr1 nuclear localisation and the actomyosin structures we examined the nuclear localisation mutant Phactr1-xxxK3A KRE/3A, which is nuclear in only a small proportion of expressing cells. Cells exhibiting predominantly nuclear Phactr1-xxxK3A KRE/3A

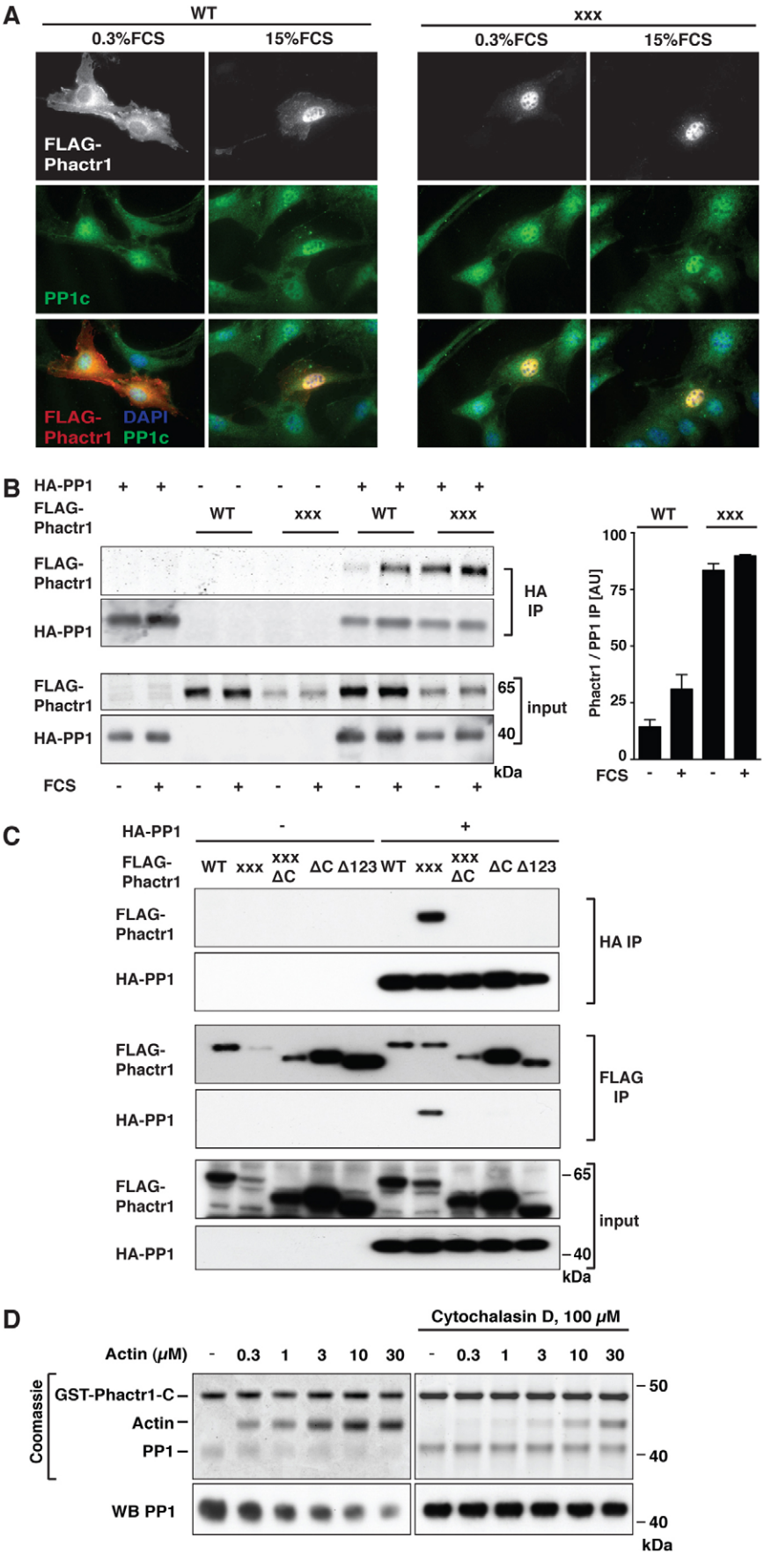

Fig. 4. Actin and PP1 bind competitively to Phactr1. (**A**) Subcellular localisation of PP1. PP1 was visualised by fluorescence microscopy in cells transfected with FLAG-tagged Phactr1WT or Phactr1-xxx before and after serum stimulation. WT, wild-type. (**B**) Nuclear accumulation of Phactr1 correlates with increased PP1 binding. Cells were transfected with wild-type Phactr1 or Phactr1-xxx and HA-tagged PP1, and interaction between PP1 and Phactr1 before and after serum stimulation monitored by quantitative immunoblotting of immunoprecipitates with FLAG and HA antibodies using ImageQuant Analysis Software (AU, arbitrary units). (**C**) Phactr1–PP1 interaction requires both RPEL domain sequences and the conserved C-terminal sequences. Interaction between the indicated Phactr1 mutants (see Fig. 2B) and PP1 in serum-starved cells was monitored by co-immunoprecipitation assay as in B. (**D**) G-actin competes directly with PP1 for Phactr1 binding. GST-Phactr1 392C and PP1 were co-expressed in bacteria. The resulting complex was purified and incubated with increasing amounts of LatB–actin in the presence or absence of 100 μM cytochalasin D. GST-Phactr1 392C-bound proteins were recovered by pulldown and analysed by Coomassie blue staining (upper) or immunoblotting (lower).

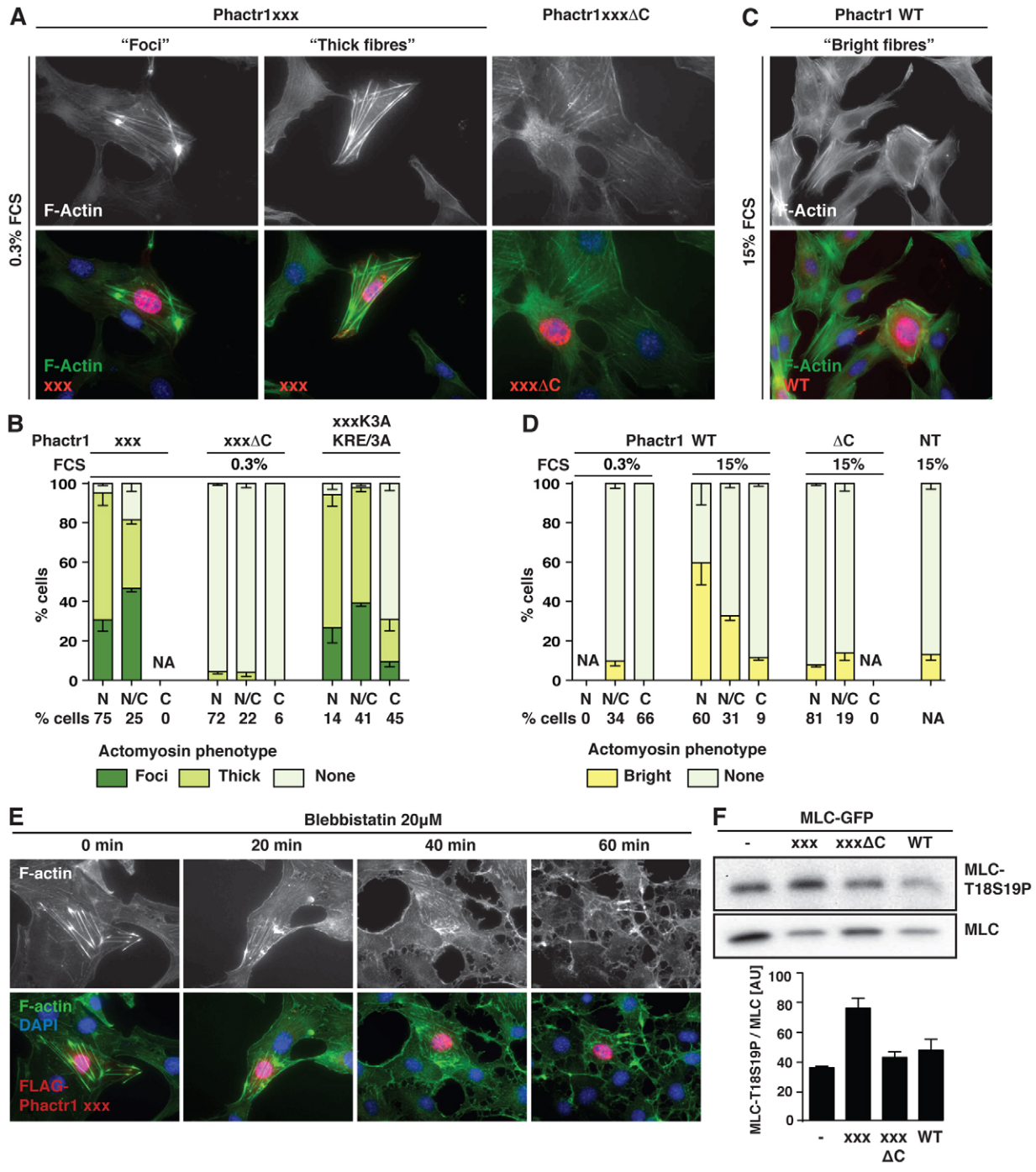

Fig. 5. Nuclear Phactr1 induces aberrant actomyosin assembly in fibroblasts. (**A**) NIH3T3 cells transfected with the indicated FLAG-tagged Phactr1 derivatives were maintained in 0.3% FCS for 20 hours before visualisation of Phactr1 and F-actin by fluorescence microscopy. The actomyosin phenotypes were scored as 'Foci', 'Thick Fibres' or none; specimen phenotypes in cells expressing Phactr1-xxx and Phactr1-xxxΔC are shown. Further examples are shown in supplementary material Fig. S5A. (**B**) Quantitation of cytoskeletal phenotypes in cells expressing Phactr1-xxx derivatives scored according to Phactr1 subcellular localisation (N, N/C or C as in Fig. 1; 100 cells per experiment; error bars, s.e.m. of three independent experiments; NA, not applicable). Specimen images for the Phactr1-xxxK3A–KRE/3A mutant are shown in supplementary material Fig. S8. (**C**) 'Bright-fibre' F-actin phenotype in NIH3T3 cells expressing wild-type Phactr1 after 1 hour serum stimulation. Further examples are shown in supplementary material Fig. S9. WT, wild-type. (**D**) Quantitation of 'bright-fibre' phenotypes in cells expressing Phactr1-WT or Phactr1ΔC, scored as in B. Phenotypes of serum-stimulated untransfected cells (NT) are scored on the right. (**E**) Rapid dispersal of aberrant F-actin structures in Phactr1-xxx-expressing NIH3T3 cells following treatment with 20 μM blebbistatin. (**F**) Phactr1-xxx expression increases MLC-T18S19 phosphorylation. NIH3T3 cells expressing the indicated FLAG-tagged Phactr1 derivatives and MLC-GFP were maintained in 0.3% FCS, and cell lysates were analysed by quantitative immunoblotting using anti-Phospho-MLC2 (T18/S19) and anti-MLC2 antibodies (AU, arbitrary units). Note that Phactr1-xxx is expressed at a significantly lower level (supplementary material Fig. S3). Error bars represent the s.e.m. of three independent experiments.

localisation exhibited a greater preponderance of aberrant actomyosin structures than those in which it was predominantly cytoplasmic (Fig. 5B; supplementary material Fig. S8). We also assessed actomyosin structures in cells expressing wild-type Phactr1 before and after serum stimulation. Following serum stimulation and Phactr1 nuclear accumulation, no foci were observed, but a significant proportion of the cells exhibited a 'bright fibre' phenotype, which is similar to but less pronounced than the 'thick fibre' phenotype, and was seen at only low frequency in untransfected cells (Fig. 5C,D; supplementary material Fig. S9).

Consistent with the presence of MLC in the aberrant F-actin structures, they dispersed rapidly following treatment of the cells with the myosin II ATPase inhibitor blebbistatin (Kovács et al., 2004) (Fig. 5E). ROCK potentiates actomyosin contractility by inactivating MLC phosphatase and possibly by direct phosphorylation of MLC (Kimura et al., 1996; Narumiya et al., 2009). Consistent with this, the proportion of co-expressed MLC-GFP phosphorylated at T18 and S19 was increased twofold by Phactr1-xxx expression (Fig. 5F). Taken together with the increased PP1 binding by activated nuclear Phactr1, this suggests that nuclear Phactr1 interacts with PP1 to induce MLC phosphorylation and aberrant actomyosin assembly (see Discussion).

Serum-regulated Phactr1 nuclear accumulation and PP1 interaction in CHL-1 melanoma cells

The preceding experiments demonstrate that Phactr1 subcellular localisation and PP1 interaction can be regulated by Rho-actin signalling in fibroblasts, and establish a potential role for G-actin–Phactr1 interaction in control of actomyosin contractility. Phactr1 is highly expressed in cells and tissues of neuronal origin (Allen et al., 2004), and its expression is associated with poor prognosis in melanoma, a neural crest-derived tumour (Smith et al., 2005; Koh et al., 2009; Trufant, 2010). We therefore studied Phactr1 in CHL-1 melanoma cells. Serum stimulation of CHL-1 cells induced nuclear accumulation of endogenous Phactr1 (Fig. 6A). As seen in transfected fibroblasts, mutation of the C-terminal RPEL motifs resulted in constitutively nuclear localisation of Phactr1 in CHL-1 cells (Fig. 6B). Nuclear accumulation of endogenous Phactr1 was accompanied by increased PP1 binding, as assessed by the increased recovery of endogenous Phactr1 in PP1 immunoprecipitates following serum stimulation (Fig. 6C). Phactr1 thus exhibits actin-regulated nucleocytoplasmic shuttling and PP1 binding in melanoma cells.

Phactr1 is required for cytoskeletal dynamics and invasion in melanoma cells

To assess the functional significance of Phactr1 for regulation of the actin cytoskeleton and cell motility in CHL-1 cells, we employed RNAi-mediated Phactr1 depletion. Phactr1 protein levels were substantially reduced in CHL-1 cells transfected with Phactr1 siRNA pool of four oligonucleotides (supplementary material Fig. S10A). Deconvolution identified three active siRNAs, which were combined for use in further experiments (supplementary material Fig. S10B). Depletion of Phactr1 greatly

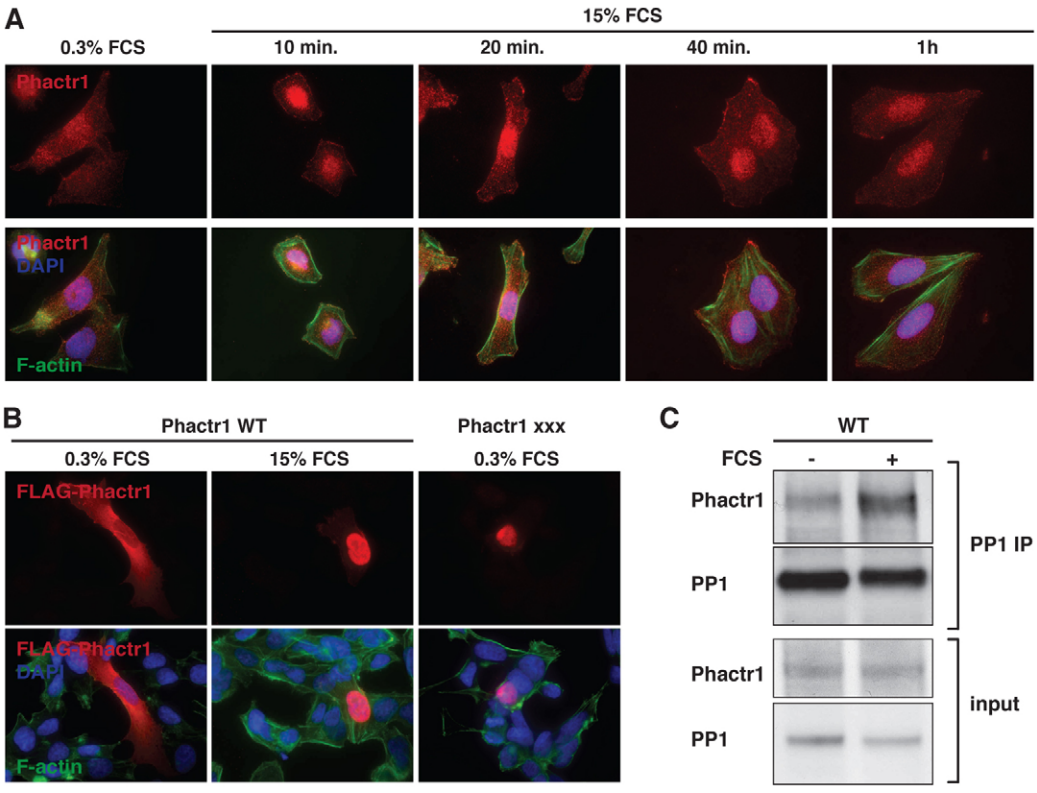

Fig. 6. Signal-controlled Phactr1 nuclear accumulation and PP1 binding in CHL-1 melanoma cells. (**A**) Cells were maintained in 0.3% FCS for 20 hours, stimulated with 15% FCS, and endogenous Phactr1 visualised by fluorescence microscopy. (**B**) Cells were transfected with the indicated Phactr1 derivatives (see Fig. 2B) and maintained in 0.3% FCS for 20 hours, with 1 hour serum stimulation as indicated, before visualisation of Phactr1 by fluorescence microscopy. (**C**) PP1 immunoprecipitates from CHL-1 cells maintained in 0.3% serum for 20 hours with or without a 1 hour serum stimulation were analysed by immunoblotting for endogenous Phactr1 and endogenous PP1.

reduced the number of transverse stress fibres in CHL-1 cells, although cortical F-actin persisted; paxillin staining indicated that their associated focal adhesions were replaced by a greater number of smaller structures dispersed around the cell periphery (Fig. 7A). Similar results were seen with the separate Phactr1 siRNA oligonucleotides (supplementary material Fig. S10C). Thus, it appears that Phactr1 is required for stress fibre assembly in CHL-1 cells, consistent with the ability of the constitutively active Phactr1-xxx to induce actomyosin foci in fibroblasts.

Given the effects of Phactr1 on cytoskeletal dynamics, we evaluated the role of Phactr1 in motile and invasive behaviour. In the scratch-wound motility assay, Phactr1-depleted CHL-1 cells moved both more slowly and with less directionality than control cells (Fig. 7B). Depletion of Phactr1 also reduced the ability of CHL-1 cells to invade through matrigel and collagen matrices (Fig. 7C and data not shown). Taken together these results indicate that in CHL-1 melanoma cells, Phactr1 activity is required for actomyosin assembly, motility and invasiveness.

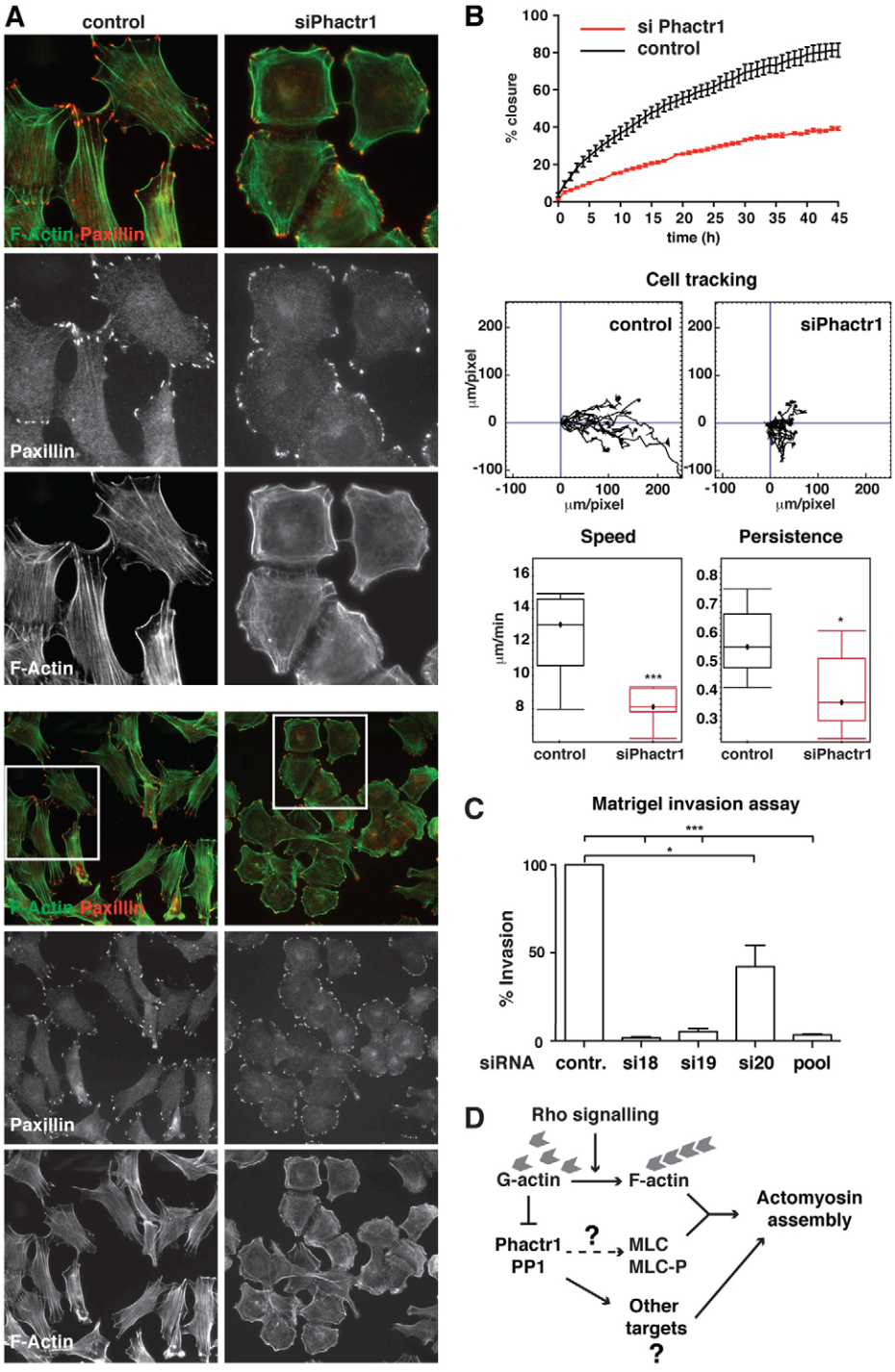

Fig. 7. Phactr1 is required for contractility, motility and invasiveness in CHL-1 melanoma cells. (**A**) Morphological changes and actin stress fibre dispersal following Phactr1 knockdown. F-actin and paxillin were visualised by immunofluorescence in cells treated with control siRNA or the three active Phactr1 siRNA oligonucleotides used in combination. Upper panels show single cell fields (65×) from the larger fields (25×) in the lower panels. Supplementary material Fig. S10 presents similar results with the individual Phactr1 siRNAs. (**B**) Phactr1 knockdown impairs cell motility. Cells were treated with control or the Phactr1 siRNA pool and grown to confluence. A scratch was made across the monolayer and migration of individual cells tracked over 45 hours using video microscopy. Top, time course of wound closure; middle, tracks of 10 individual cells from each population; bottom, migration speed and persistence. Statistical significance was assessed by ANOVA (*P<0.05; ***P<0.001). (**C**) Phactr1 knockdown reduces invasiveness. Cells treated with control, individual Phactr1 siRNAs or the Phactr1 siRNA pool were allowed to migrate through a matrigel-coated filter towards serum-containing medium for 22 hours, and cells that had traversed the filter were then imaged. Efficiency of migration was expressed relative to control cells. Error bars represent the s.e.m. of three independent experiments, 16 images per experiment. Statistical significance was assessed by paired t-test (*P<0.05; ***P<0.001). (**D**) Potential homeostatic role for Phactr1 in coordination of actomyosin assembly with F-actin availability. Actin represses the ability of nuclear Phactr1 to interact with PP1 and promote actomyosin assembly. The nature of the link to MLC phosphorylation might be direct, perhaps by inhibiting MLCP, or indirect, through other pathways. For discussion see text.

Discussion

In this paper we have uncovered roles for G-actin binding in the regulation of the RPEL protein Phactr1. Signal-induced depletion of the G-actin pool induces Phactr1 nuclear accumulation in both fibroblasts and melanoma cells. G-actin regulates importin α-β binding to two nuclear import signals associated with the RPEL motifs of the protein. Interaction of G-actin with the C-terminal RPEL repeat of Phactr1 inhibits binding of PP1, which interacts with the Phactr1 conserved C-terminus and sequences within the RPEL domain, as previously shown for Phactr3 (Sagara et al., 2003). Activation of wild-type Phactr1 induces assembly of actomyosin structures, while actomyosin foci and thickened stress fibres are induced by a mutant form of Phactr1 that is constitutively nuclear and cannot bind actin. Conversely, downregulation of Phactr1 in a melanoma cell line decreased actomyosin assembly, motility and invasiveness. High Phactr1 expression is associated with poor prognosis in melanoma (Smith et al., 2005; Koh et al., 2009) and melanoma from nevi (Trufant, 2010), and we speculate this may reflect the role of Phactr1 in invasive and motile behaviour (Sahai and Marshall, 2002; Narumiya et al., 2009).

Phactr1 appears to be the only member of the Phactr family that undergoes regulated nuclear accumulation in response to Rho-actin signalling. Regulated nuclear accumulation of the MRTF family of RPEL proteins plays a critical part in their role as coactivators of their partner transcription factor SRF (Miralles et al., 2003; Vartiainen et al., 2007). Two lines of evidence indicate that induction of the actomyosin phenotypes is the consequence of Phactr1 interaction with PP1 in the nucleus. First, the activated mutant Phactr1-xxx, which cannot bind actin, is constitutively nuclear, and requires PP1 binding to induce actomyosin assembly. In contrast, import-defective Phactr1-xxx derivatives cannot effectively induce the actomyosin phenotype when located in the cytoplasm. Second, overexpression of wild-type Phactr1 does not induce actomyosin assembly unless relocated to the nucleus by serum stimulation, and this also requires PP1 binding. However, in melanoma cells, even under unstimulated conditions when Phactr1 is predominantly cytoplasmic, its depletion disperses stress fibres, consistent with either an additional cytoplasmic target or with Phactr1 continuously shuttling through the nucleus, as observed with the MRTFs (Vartiainen et al., 2007).

In contrast to Phactr1, we found that Phactr2, Phactr3 and Phactr4 did not exhibit actin-regulated nuclear accumulation. Work is in progress to determine the basis for this differential regulation, which may reflect differences in G-actin binding properties, nuclear import and export elements, or both. In the other Phactr proteins, the affinity of RPEL3 is always comparable with that of Phactr1, but in each protein one of the other RPEL motifs exhibits substantially lower affinity than its Phactr1 counterpart (Mouilleron et al., 2012). RPEL3 overlaps the PP1-binding region, at least in Phactr3 (Sagara et al., 2003), and our data therefore suggest that the other family members will still exhibit actin-regulated interaction with PP1. We favour the idea that G-actin governs the interaction of Phactr2, Phactr3 and Phactr4 with local PP1 populations. It will be interesting to investigate the effects of disrupting the interactions between these family members and G-actin.

The non-actin binding Phactr1 mutant Phactr1-xxx induces formation of actomyosin foci and thickened actin stress fibres reminiscent of those induced by activated ROCK (Leung et al., 1996; Sahai et al., 1998), with concomitant accumulation of phosphorylated myosin light chain. Serum-induced nuclear accumulation of wildtype Phactr1 also induces actomyosin rearrangements. Conversely, in melanoma cells, depletion of Phactr1 results in dispersion of stress fibres, cell spreading, and decreased cell speed and persistence in the scratch-wound assay. These results suggest that Phactr1 promotes actomyosin contractility, and that this reflects at least in part increased MLC phosphorylation. According to this view, the regulation of Phactr1 activity by G-actin would effectively provide a homeostatic feedback loop serving to coordinate levels of phosphorylated MLC, and hence actomyosin crosslinking, with F-actin assembly (Fig. 7D). Interestingly, G-actin-mediated control of the MRTFs, another RPEL protein family, also provides a homeostatic feedback loop which allows the coordination of cytoskeletal gene expression with cytoskeletal dynamics (Medjkane et al., 2009; Olson and Nordheim, 2010).

Regulation of the activity of MLC phosphatase, a PP1 complex, plays an important part in the control of MLC phosphorylation (for review, see Somlyo and Somlyo, 2003). PP1 holoenzymes comprise catalytic core subunits associated with one or more regulatory subunits, which either act positively to refine PP1 substrate specificity or as substrate-independent inhibitory cofactors (for reviews, see Ceulemans and Bollen, 2004; Bollen et al., 2010). While our data show that nuclear Phactr1-PP1 interaction promotes MLC phosphorylation, leading to actomyosin assembly, the mechanism remains unclear. In principle, Phactr1 could act directly, as an MLCP inhibitor. Given the cytoplasmic location of MLCP it is perhaps more likely that it acts indirectly, although MYPT–PP1 complexes have been reported to mediate nuclear events (Kiss et al., 2008; Bollen et al., 2010). For example, nuclear Phactr1 might act positively as part of a PP1 holoenzyme regulating pathways indirectly controlling levels of phosphorylated MLC (Fig. 7D). In this regard studies of the mouse Phactr4 *humdy* mutation have led to the proposal that Phactr4–PP1 complexes act positively to dephosphorylate pRb and cofilin in different cell contexts (Kim et al., 2007; Zhang et al., 2012), although this has yet to be confirmed by a direct test. Structural studies of the Phactr1–PP1 complex may shed light on the functional consequences of its interaction with PP1. It also remains possible that Phactr1 controls targets other than MLC to rearrange actomyosin structures, perhaps even via effects on gene expression, and work is under way to address these issues.

Rho-actin signalling controls the subcellular localisation of Phactr1, with lowered G-actin levels causing nuclear accumulation, and elevated levels inhibiting it. By analogy with the MRTF family of RPEL domain proteins, this is likely to reflect alterations in G-actin loading onto the regulatory RPEL motifs (Vartiainen et al., 2007). Our data indicate that cytoplasmic localisation in resting cells requires actin binding to the Phactr1 C-terminal RPEL repeat, but not to its N-terminal RPEL-N motif. We show elsewhere that the Phactr1 C-terminal RPEL repeat assembles a trivalent actin–RPEL complex, with actins bound to each of its three RPEL motifs (Mouilleron et al., 2012). In contrast, the MRTF repeat assembles a pentavalent complex, with G-actins binding the RPEL motifs and the intervening spacers, and all of these actin binding sites are required for cytoplasmic localisation of MRTF in resting cells (Guettler et al., 2008; Mouilleron et al., 2008; Mouilleron et al., 2011). Nevertheless, our results indicate that the Phactr1 and MRTF actin–RPEL assemblies respond in a similar fashion to

variations in G-actin concentration. We are currently investigating the binding kinetics of G-actin to the different RPEL domains.

Nuclear import of Phactr1 is importin α-β dependent, but unlike the MRTFs, its export from the nucleus is independent of Crm1. Two Phactr1 NLS elements are located adjacent to the N-terminal RPEL-N motif, and within the C-terminal RPEL domain, and G-actin competes with importin α-β for binding to these elements. Consistent with this, we found that artificial elevation of cellular G-actin concentrations can inhibit serum-induced Phactr1 nuclear accumulation, and this requires both the N-terminal RPEL motif and the C-terminal RPEL repeat. We propose that the inhibited state involves saturation of all the Phactr1 actin-binding sites and occlusion of their associated nuclear import signals. This is likely to reflect formation of a tetravalent actin–RPEL complex through cooperative interactions between the actin-bound RPEL-N motif and a trivalent actin–RPEL assembly on the C-terminal domain (Mouilleron et al., 2012). Elevated actin concentrations also inhibit MRTF nuclear import (Vartiainen et al., 2007), but in this case the inhibited state is likely to reflect saturation of its RPEL domain by the pentavalent actin–RPEL complex, which effectively occludes the MRTF importin α-β binding site (Pawlowski et al., 2010; Hirano and Matsuura, 2011; Mouilleron et al., 2011).

Our studies have revealed functional roles for G-actin in control of Phactr1 nucleocytoplasmic shuttling and PP1 interaction. The findings emphasise the significance of the RPEL motif in allowing modulation of protein interactions according to G-actin concentration. While the MRTFs and Phactr protein families exhibit differing arrangements of RPEL motifs, their activities, at least in nucleocytoplasmic shuttling, nevertheless respond similarly to variations in G-actin concentration. It will be interesting to see if other G-actin binding motifs are exploited to allow actin-dependent control of protein interactions and localisation.

Materials and Methods

Plasmids

Sequences containing mouse cDNA for Phactr1, Phactr2, Phactr3 or Phactr4 were inserted into a pEF-Flag vector for mammalian expression using primers: Phactr1 5′-atggattatcccaaaatggat-3′ and 5′-ttaaggtcgatgaaacctggt-3′; Phactr2 5′-atgggcca-gacctcggtgtcc-3′ and 5′-ttatggacgatgaaaccttgt-3′; Phactr3 5′-atggccgcatccgaggac-ggc-3′ and 5′-ctatggcctgtggaatcttgt-3′; Phactr4 5′-atggaagacccatcggaagaa-3′ and 5′-tcatgggcgatggtagcgtgt-3′. For Phactr1 derivatives see supplementary material Table S1. PP1 was inserted into pEF-HA vector for mammalian expression using primers 5′-atgtccgacagcgagaagctc-3′ and 5′-ctatttcttggctttggcaga-3′. Expression plasmids for C3 transferase, WT actin, R62D actin and MLC-GFP have been described previously (Posern et al., 2002; Miralles et al., 2003; Wyckoff et al., 2006).

Proteins and peptides

Actin was prepared from rabbit skeletal muscle as described earlier (Feuer et al., 1948; Spudich and Watt, 1971) and bound to latrunculin B as described (Mouilleron et al., 2008). N-terminally FITC-conjugated peptides were synthesised and HPLC-purified by the Cancer Research UK Protein and Peptide Chemistry Laboratory (for sequences see supplementary material Table S2). Fluorescence polarisation was measured and fluorescence anisotropy calculated as previously described (Mouilleron et al., 2008).

Transfections, immunofluorescence microscopy and immunoblotting

Mouse NIH3T3 fibroblasts and human MDA-MB-231 breast carcinoma cells were maintained in DMEM with 10% fetal calf serum (FCS), and CHL-1 human melanoma cells in RPMI containing 10% FCS. NIH3T3, CHL-1 or MDA-MB-231 cells (150,000 cells per well in a six-well dish) were transfected with expression plasmid using Lipofectamine 2000 (Invitrogen) according to the manufacturer's instructions. For serum stimulation experiments cells were maintained in medium containing 0.3% FCS for 20 hours and then stimulated with 15% FCS. Inhibitor treatments were 30 nM LMB, 1 μM LatB, 10 μM Y27632, 10 μM CD or 20 μM blebbistatin. Immunofluorescence microscopy was performed as described earlier (Vartiainen et al., 2007; Guettler et al., 2008). F-actin was detected with FITC-phalloidin (Invitrogen) and nuclei were visualised using DAPI. SDS-PAGE analysis of cell lysates and immunoblotting was performed using standard techniques and quantified using ImageQuant Analysis Software. Primary antibodies were anti-FLAG (Sigma F7425), HA (3F10, Roche), Phactr1 (SIGMA HPA029756), MLC2 (3672, Cell Signaling), Phospho-MLC2(T18/S19) (3674, Cell Signalling), PP1α (C-19, Santa-Cruz), Actin (C-4, Santa-Cruz), α-Tubulin (T5168, Sigma), GST (G7781, Sigma), Importin α (BD Transduction Laboratories), Importin β (ab45938, Abcam). For Phactr1 immunoblotting nitrocellulose membranes were preincubated in Superblock (Thermo Scientific) overnight, probed with Phactr1 antibody in Superblock (1:250) for 2 hours, and washed five times with TBST. Secondary antibodies were diluted in Superblock (1:10,000).

Fluorescence anisotropy

Fluorescence anisotropy assays were performed essentially as described (Guettler et al., 2008; Mouilleron et al., 2008). Dissociation constants (K_d) were calculated by nonlinear regression in Prism software using equation: $Y=((A_b-A_f)*(X/(K_d+X))) + A_f$ (Heyduk and Lee, 1990), where X is protein concentration, Y is total anisotropy, A_b is anisotropy from bound ligand, A_f is anisotropy from free ligand. K_d values were derived from duplicate samples in three independent experiments.

RNAi-mediated protein depletion

For wound healing assay CHL-1 cells were plated onto 96-well plates (5000 cells/well), for immunoblotting and immunofluorescence CHL-1 cells were plated onto six-well plates (150,000 cells/well). siRNA transfections used 20 nM siRNA with Lipofectamine RNAiMAX (Invitrogen) according to the manufacturer's instructions. For Phactr1, cells were treated with 20 nM Dharmacon Phactr1 ON-TARGETplus SMARTpool siRNA. Deconvolution experiments identified sequences J-025063-18, J-025063-19 and J-025063-20 as effective (supplementary material Fig. S10), which were used in combination (20 nM each) unless otherwise stated. Other siRNAs used were mouse importin β siRNA (Dharmacon, L-058740-00) or AllStars negative control (Qiagen). After 72 hours, cells were processed for immunoblotting, microscopy or migration assays.

Co-immunoprecipitation

Cells transfected with FLAG-Phactr1 derivatives and/or HA-PP1 were lysed in 0.5% Nonidet P-40, 1 mM EDTA, 50 mM Tris, pH 8.0, 120 mM NaCl, 0.1 mM sodium vanadate, 1 tablet/50 ml protease inhibitors cocktail (Roche). Total protein (1 mg) was used for immunoprecipitation with Anti-HA-agarose (A2095 SIGMA) or Anti-FLAG M1 agarose affinity gel (A4596 SIGMA). After four washes in lysis buffer, proteins were separated by SDS-PAGE and immunoblotted using standard techniques. For endogenous proteins in CHL1 cells, lysis was in 20 mM Tris.HCl pH 7.4, 150 mM NaCl, 0.1% (w/v) SDS, 0.5% (w/v) Na-deoxycholate, 1% (v/v) Triton X-100, 1 tablet per 50 ml Roche Complete, 1.0 mM PMSF. For immunoprecipitation, 1 μg PP1α antibody was used per 500 μg lysate.

GST pulldown assays

For GST pulldown experiments, glutathione-sepharose was saturated with GST-Phactr1 N-terminal (1–171) or C-terminal (392–580) derivatives from bacterial lysates. The beads were then washed and incubated with purified recombinant importins α3 and β1. PP1 protein was directly co-expressed with GST-Phactr1-C in bacteria and the resulting complex was purified using the previously described protocol for PP1 purification (Kelker et al., 2009). The pulldown of Phactr1 with either importin α-β or PP1 were performed for 1 hour at 4℃ in the respective binding buffers: (50 mM Tris pH 7.8, 50 mM NaCl, 5 mM $MgCl_2$) and (20 mM Tris pH 8.0, 100 mM NaCl, 0.5% Triton X-100, 5 mM $MgCl_2$, 0.5 mM $MnCl_2$, 0.2 mM EGTA, 0.2 mM ATP, 1 mM DTT). The resin was then washed four times with binding buffer, resuspended in SDS loading buffer and the supernatant was subjected to 4–12% SDS-PAGE. Proteins were stained with Coomassie Brilliant Blue or analysed by immunoblotting.

Scratch-wound assays

Confluent cells were scratch-wounded in 96-well plates using Woundmaker 96 (Essen BioScience). Cell migration was monitored using IncuCyte™ (Essen BioScience) video microscopy every 30 minutes for 48 hours after scratching. Cells at the leading edge of the scratch were tracked using Tracker software. Mean speeds were calculated over the recording time for each cell; persistence was measured during successive 50-minute windows for each cell. Migration speed and persistence were evaluated using an algorithm implemented in Mathematica software (Wolfram Research), with hierarchical ANOVA analysis as described previously (Medjkane et al., 2009).

Matrigel invasion assay

72 hours post-transfection, siRNA-treated cells were transferred to duplicate wells (2×10^4 cells/well) of a BD Matrigel^{TM} Invasion Chamber (24-well plate, 8.0 micron; BD Biosciences) in serum-free medium, and allowed to migrate through the matrigel-coated filter towards full medium. After 22 hours, cells on both sides of the wells were fixed with 4% PFA and stained with Phalloidin Alexa-488 and DAPI. Cells which had migrated through the filter (visualised by reflection microscopy) were imaged using a LSM 510 Zeiss confocal microscope (20× lens; 16 images per well). Migration was assessed relative to control siRNA-treated cells.

Acknowledgements

We thank Nicola O'Reilly and the LRI peptide synthesis group for peptides, the LRI light microscopy facility for advice and support, and Rafal Pawlowski and Erik Sahai for helpful discussions and advice. M.W. and J.D. isolated, manipulated and expressed cDNAs and designed and performed protein localisation experiments. J.D. performed protein interactions studies. J.A. and M.W. performed cell biology studies. M.W. and S.M. performed protein expression experiments. N.Q.M. and M. Way contributed to experimental design. RT conceived the project, contributed to experimental design and interpretation, and drafted the paper with M.W. All authors contributed to development of the manuscript. The authors have no conflicts of interest.

Funding

S.M. was funded by Cancer Research UK and an Advanced Investigator grant from the European Research Council (ERC) to R.T. (Project 268690). J.A. was funded by an EMBO Longterm Fellowship. This work was supported by Cancer Research UK core funding to the London Research Institute (to R.T., M.Way, N.M.) and by ERC Advanced Grant 268690 to R.T.

Supplementary material available online at
http://jcs.biologists.org/lookup/suppl/doi:10.1242/jcs.112078/-/DC1

References

Allen, P. B., Greenfield, A. T., Svenningsson, P., Haspeslagh, D. C. and Greengard, P. (2004). Phactrs 1-4: A family of protein phosphatase 1 and actin regulatory proteins. *Proc. Natl. Acad. Sci. USA* **101**, 7187-7192.

Bankovic, J., Stojsic, J., Jovanovic, D., Andjelkovic, T., Milinkovic, V., Ruzdijic, S. and Tanic, N. (2010). Identification of genes associated with non-small-cell lung cancer promotion and progression. *Lung Cancer* **67**, 151-159.

Bollen, M., Peti, W., Ragusa, M. J. and Beullens, M. (2010). The extended PP1 toolkit: designed to create specificity. *Trends Biochem. Sci.* **35**, 450-458.

Ceulemans, H. and Bollen, M. (2004). Functional diversity of protein phosphatase-1, a cellular economizer and reset button. *Physiol. Rev.* **84**, 1-39.

Dominguez, R. and Holmes, K. C. (2011). Actin structure and function. *Annu. Rev. Biophys.* **40**, 169-186.

Farghaian, H., Chen, Y., Fu, A. W., Fu, A. K., Ip, J. P., Ip, N. Y., Turnley, A. M. and Cole, A. R. (2011). Scapinin-induced inhibition of axon elongation is attenuated by phosphorylation and translocation to the cytoplasm. *J. Biol. Chem.* **286**, 19724-19734.

Favot, L., Gillingwater, M., Scott, C. and Kemp, P. R. (2005). Overexpression of a family of RPEL proteins modifies cell shape. *FEBS Lett.* **579**, 100-104.

Feuer, G., Molnar, F., Pettko, E. and Straub, F. B. (1948). Studies on the composition and polymerization of actin. *Hung. Acta Physiol.* **1**, 150-163.

Gieni, R. S. and Hendzel, M. J. (2009). Actin dynamics and functions in the interphase nucleus: moving toward an understanding of nuclear polymeric actin. *Biochem. Cell Biol.* **87**, 283-306.

Guettler, S., Vartiainen, M. K., Miralles, F., Larijani, B. and Treisman, R. (2008). RPEL motifs link the serum response factor cofactor MAL but not myocardin to Rho signaling via actin binding. *Mol. Cell. Biol.* **28**, 732-742.

Heyduk, T. and Lee, J. C. (1990). Application of fluorescence energy transfer and polarization to monitor *Escherichia coli* cAMP receptor protein and lac promoter interaction. *Proc. Natl. Acad. Sci. USA* **87**, 1744-1748.

Hirano, H. and Matsuura, Y. (2011). Sensing actin dynamics: structural basis for G-actin-sensitive nuclear import of MAL. *Biochem. Biophys. Res. Commun.* **414**, 373-378.

Jarray, R., Allain, B., Borriello, L., Biard, D., Loukaci, A., Larghero, J., Hadj-Slimane, R., Garbay, C., Lepelletier, Y. and Raynaud, F. (2011). Depletion of the novel protein PHACTR-1 from human endothelial cells abolishes tube formation and induces cell death receptor apoptosis. *Biochimie* **93**, 1668-1675.

Kathiresan, S., Voight, B. F., Purcell, S., Musunuru, K., Ardissino, D., Mannucci, P. M., Anand, S., Engert, J. C., Samani, N. J., Schunkert, H. et al.; Myocardial Infarction Genetics Consortium; Wellcome Trust Case Control Consortium (2009). Genome-wide association of early-onset myocardial infarction with single nucleotide polymorphisms and copy number variants. *Nat. Genet.* **41**, 334-341.

Kelker, M. S., Page, R. and Peti, W. (2009). Crystal structures of protein phosphatase-1 bound to nodularin-R and tautomycin: a novel scaffold for structure-based drug design of serine/threonine phosphatase inhibitors. *J. Mol. Biol.* **385**, 11-21.

Kim, T. H., Goodman, J., Anderson, K. V. and Niswander, L. (2007). Phactr4 regulates neural tube and optic fissure closure by controlling PP1-, Rb-, and E2F1-regulated cell-cycle progression. *Dev. Cell* **13**, 87-102.

Kimura, K., Ito, M., Amano, M., Chihara, K., Fukata, Y., Nakafuku, M., Yamamori, B., Feng, J., Nakano, T., Okawa, K. et al. (1996). Regulation of myosin phosphatase by Rho and Rho-associated kinase (Rho-kinase). *Science* **273**, 245-248.

Kiss, A., Lontay, B., Bécsi, B., Márkász, L., Oláh, E., Gergely, P. and Erdodi, F. (2008). Myosin phosphatase interacts with and dephosphorylates the retinoblastoma protein in THP-1 leukemic cells: its inhibition is involved in the attenuation of daunorubicin-induced cell death by calyculin-A. *Cell. Signal.* **20**, 2059-2070.

Koh, S. S., Opel, M. L., Wei, J. P., Yau, K., Shah, R., Gorre, M. E., Whitman, E., Shitabata, P. K., Tao, Y., Cochran, A. J. et al. (2009). Molecular classification of melanomas and nevi using gene expression microarray signatures and formalin-fixed and paraffin-embedded tissue. *Mod. Pathol.* **22**, 538-546.

Kovács, M., Tóth, J., Hetényi, C., Málnási-Csizmadia, A. and Sellers, J. R. (2004). Mechanism of blebbistatin inhibition of myosin II. *J. Biol. Chem.* **279**, 35557-35563.

Leung, T., Chen, X. Q., Manser, E. and Lim, L. (1996). The p160 RhoA-binding kinase ROK alpha is a member of a kinase family and is involved in the reorganization of the cytoskeleton. *Mol. Cell. Biol.* **16**, 5313-5327.

Medjkane, S., Perez-Sanchez, C., Gaggioli, C., Sahai, E. and Treisman, R. (2009). Myocardin-related transcription factors and SRF are required for cytoskeletal dynamics and experimental metastasis. *Nat. Cell Biol.* **11**, 257-268.

Miralles, F., Posern, G., Zaromytidou, A. I. and Treisman, R. (2003). Actin dynamics control SRF activity by regulation of its coactivator MAL. *Cell* **113**, 329-342.

Mouilleron, S., Guettler, S., Langer, C. A., Treisman, R. and McDonald, N. Q. (2008). Molecular basis for G-actin binding to RPEL motifs from the serum response factor coactivator MAL. *EMBO J.* **27**, 3198-3208.

Mouilleron, S., Langer, C. A., Guettler, S., McDonald, N. Q. and Treisman, R. (2011). Structure of a pentavalent G-actin*MRTF-A complex reveals how G-actin controls nucleocytoplasmic shuttling of a transcriptional coactivator. *Sci. Signal.* **4**, ra40.

Mouilleron, S., Wiezlak, M., O'Reilly, N., Treisman, R. and McDonald, N. Q. (2012). Structures of the Phactr1 RPEL domain and RPEL motif complexes with G-actin reveal the molecular basis for actin binding cooperativity. *Structure* **20**, 1960-1970.

Nair, U. B., Joel, P. B., Wan, Q., Lowey, S., Rould, M. A. and Trybus, K. M. (2008). Crystal structures of monomeric actin bound to cytochalasin D. *J. Mol. Biol.* **384**, 848-864.

Narumiya, S., Tanji, M. and Ishizaki, T. (2009). Rho signaling, ROCK and mDia1, in transformation, metastasis and invasion. *Cancer Metastasis Rev.* **28**, 65-76.

Olson, E. N. and Nordheim, A. (2010). Linking actin dynamics and gene transcription to drive cellular motile functions. *Nat. Rev. Mol. Cell Biol.* **11**, 353-365.

Pawlowski, R., Rajakylä, E. K., Vartiainen, M. K. and Treisman, R. (2010). An actin-regulated importin α/β-dependent extended bipartite NLS directs nuclear import of MRTF-A. *EMBO J.* **29**, 3448-3458.

Posern, G., Sotiropoulos, A. and Treisman, R. (2002). Mutant actins demonstrate a role for unpolymerized actin in control of transcription by serum response factor. *Mol. Biol. Cell* **13**, 4167-4178.

Rost, B., Yachdav, G. and Liu, J. (2004). The PredictProtein server. *Nucleic Acids Res.* **32**, W321-W326.

Roy, J. and Cyert, M. S. (2009). Cracking the phosphatase code: docking interactions determine substrate specificity. *Sci. Signal.* **2**, re9.

Sagara, J., Higuchi, T., Hattori, Y., Moriya, M., Sarvotham, H., Shima, H., Shirato, H., Kikuchi, K. and Taniguchi, S. (2003). Scapinin, a putative protein phosphatase-1 regulatory subunit associated with the nuclear nonchromatin structure. *J. Biol. Chem.* **278**, 45611-45619.

Sagara, J., Arata, T. and Taniguchi, S. (2009). Scapinin, the protein phosphatase 1 binding protein, enhances cell spreading and motility by interacting with the actin cytoskeleton. *PLoS ONE* **4**, e4247.

Sahai, E. and Marshall, C. J. (2002). RHO-GTPases and cancer. *Nat. Rev. Cancer* **2**, 133-142.

Sahai, E., Alberts, A. S. and Treisman, R. (1998). RhoA effector mutants reveal distinct effector pathways for cytoskeletal reorganization, SRF activation and transformation. *EMBO J.* **17**, 1350-1361.

Smith, A. P., Hoek, K. and Becker, D. (2005). Whole-genome expression profiling of the melanoma progression pathway reveals marked molecular differences between nevi/melanoma *in situ* and advanced-stage melanomas. *Cancer Biol. Ther.* **4**, 1018-1029.

Somlyo, A. P. and Somlyo, A. V. (2003). Ca2+ sensitivity of smooth muscle and nonmuscle myosin II: modulated by G proteins, kinases, and myosin phosphatase. *Physiol. Rev.* **83**, 1325-1358.

Sotiropoulos, A., Gineitis, D., Copeland, J. and Treisman, R. (1999). Signal-regulated activation of serum response factor is mediated by changes in actin dynamics. *Cell* **98**, 159-169.

Spiering, D. and Hodgson, L. (2011). Dynamics of the Rho-family small GTPases in actin regulation and motility. *Cell Adh. Migr.* **5**, 170-180.

Spudich, J. A. and Watt, S. (1971). The regulation of rabbit skeletal muscle contraction. I. Biochemical studies of the interaction of the tropomyosin-troponin complex with actin and the proteolytic fragments of myosin. *J. Biol. Chem.* **246**, 4866-4871.

Trufant, J. W. (2010). *Phactr1 as a Novel Biomarker to Distinguish Malignant Melanoma from Nevus*, MD Thesis, Yale University, CT, USA.

Vartiainen, M. K., Guettler, S., Larijani, B. and Treisman, R. (2007). Nuclear actin regulates dynamic subcellular localization and activity of the SRF cofactor MAL. *Science* **316**, 1749-1752.

Wider, C., Lincoln, S. J., Heckman, M. G., Diehl, N. N., Stone, J. T., Haugarvoll, K., Aasly, J. O., Gibson, J. M., Lynch, T., Rajput, A. et al. (2009). Phactr2 and Parkinson's disease. *Neurosci. Lett.* **453**, 9-11.

Wyckoff, J. B., Pinner, S. E., Gschmeissner, S., Condeelis, J. S. and Sahai, E. (2006). ROCK- and myosin-dependent matrix deformation enables protease-independent tumor-cell invasion *in vivo*. *Curr. Biol.* **16**, 1515-1523.

Zhang, Y., Kim, T. H. and Niswander, L. (2012). Phactr4 regulates directional migration of enteric neural crest through PP1, integrin signaling, and cofilin activity. *Genes Dev.* **26**, 69-81.

Zheng, B., Han, M., Bernier, M. and Wen, J. K. (2009). Nuclear actin and actin-binding proteins in the regulation of transcription and gene expression. *FEBS J.* **276**, 2669-2685.